Carbon Trends 5 (2021) 100129

Contents lists available at ScienceDirect

Carbon Trends

journal homepage: www.elsevier.com/locate/cartre

High friction coefficient of vertically aligned carbon-nanotubes: A molecular dynamics simulation

O. Farzadian[a,*], C. Spitas[a], K.V. Kostas[a], F. Yousefi[b]

[a] Mechanical and Aerospace Engineering, School of Engineering and Digital Sciences, Nazarbayev University, Nur-Sultan 010000, Kazakhstan
[b] Department of Physics, University of Zanjan, Zanjan, 45195-313, Iran

ARTICLE INFO

Article history:
Received 15 September 2021
Revised 5 November 2021
Accepted 8 November 2021

Keywords:
Carbon nanotube
Friction coefficient
Molecular dynamics

ABSTRACT

In this study, we perform non-equilibrium molecular dynamics simulations to study the friction coefficient between two carbon nanotubes grown vertically on two separate graphene layers, which are placed parallel to each other with one set in motion. Significantly high values of approximately 3 and 1.5 are computed for the static and dynamic friction coefficients, respectively. The effects of nanotubes overlapping length, speed of relative movement on the dynamic friction coefficient are also studied in our work. According to our results, and in agreement with the standard model of friction, dynamic friction between the two carbon nanotubes remains constant, regardless of the relative speed of their movement.

1. Introduction

Carbon nanotubes (CNTs) constitute one of the most interesting and promising carbon allotropes due to their remarkable chemical and mechanical properties. These properties have inspired scientists and engineers to utilize CNTs in construction and formation of composites and films [1,2], along with several other applications. CNTs can be classified into single-walled (SWCNTs) and multi-walled carbon nanotubes (MWCNTs) with the existence of chirality, and the chirality number, playing a significant role in their exhibited properties. Theoretical investigations indicate high tensile strength of about 100 GPa for SWCNTs [3,4], but due to their size, with diameters in the range of a nanometer, it is a challenge to experimentally measure mechanical properties of CNTs. Nevertheless, experimental results for Youngs modulus and tensile strength of MWCNTs have been reported at 470 and 1163 GPa, respectively; see [5,6]. Additionally, experimental studies regarding the friction coefficient between two CNTs and the friction of vertically aligned CNTs film against gold tips have been published in the past; see [7,8]. To the best of our knowledge, no molecular dynamics (MD) simulation have been published so far to computationally demonstrate these results, although there some limited relevant publications using MD simulations to analyze rotational and transnational dynamic friction of double-walled carbon nanotubes; see [9,10]. Therefore, we consider it an interesting and useful endeavor to carry out MD simulations and compare our results against these experimental results.

This research is done with the prospect of evaluating friction micro-element candidates for MEMS design. Here we consider the friction of two CNTs attached to short graphene patches; see for example [11]. Commonly, friction surfaces used in engineering rely on surface roughness and are subject to wear, while the corresponding friction coefficients are not perfectly consistent and/or engineerable. CNT friction has not been sufficiently studied in general and, to our knowledge, not at all for the purpose just described. Therefore, the present work is a feasibility study in this context and, as our results demonstrate, quite high and consistent friction coefficient values are achievable. Therefore, one may also consider applications involving an appropriate shaping of surfaces with CNTs to achieve a controlled, high frictional behavior.

Specifically, in this work, we perform MD simulations to computationally evaluate the friction coefficient between two straight CNTs which are interlocked as depicted in Fig. 1. We furthermore consider each of these two CNTs to be grown on a flat graphene substrate as shown in the same figure. We then apply a shear force to the top layer for inducing motion and estimate the friction coefficient between them using the standard model of friction. Both static and dynamic friction coefficients are considered in this study, along with the effects of the applied shear force, movement velocity and CNTs overlapping length on them.

The rest of this paper is structured as follows: Section 2 presents the problem formulation and the employed computational approach, followed by Section 3 in which our

* Corresponding author.
E-mail address: omid.farzadian@nu.edu.kz (O. Farzadian).

https://doi.org/10.1016/j.cartre.2021.100129

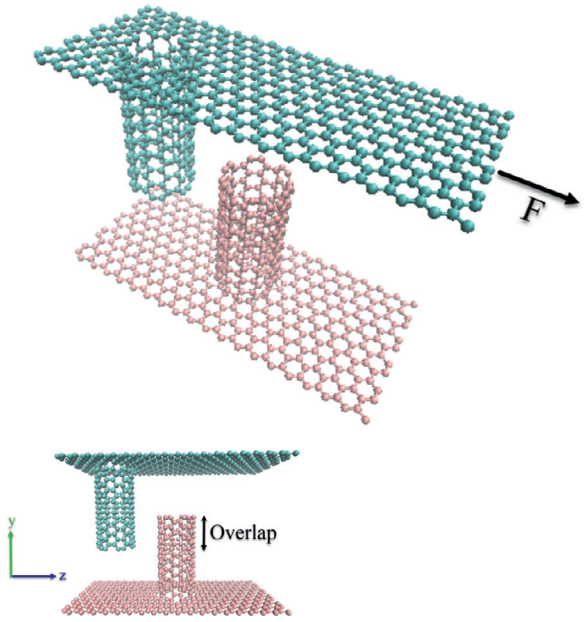

Fig. 1. The schematic of interlocked CNTs from two views. Applied force F and movement are in z direction.

simulation results are reported and discussed. Finally, concluding remarks and potential future research directions are included in Section 4.

2. Problem formulation and computational approach

Static and dynamic friction coefficients between carbon-nanotubes are calculated via non-equilibrium molecular dynamics (NEMD) simulations with periodic boundary conditions along both in-plane directions and a free boundary condition in the perpendicular direction. The present simulations consider SWCNTs of length $1-3$ nm, with (6,6) chirality (equivalent to the tube radius of ~ 0.8 nm). The optimized Tersoff potential by Lindsay and Broido [12] is considered to derive the inter-atomic forces between the carbon atoms and Verlet intergration, with a time-step of 1 fs, is employed in particles trajectory calculations. The Large-scale Atomic/ Molecular Massively Parallel Simulator (LAMMPS)[1] [13] is used for performing all molecular dynamics simulations in our work

Proper calculation of friction force requires a series of preparatory steps that are briefly described here. First, energy minimization is performed for positioning atoms in the system. Then, we implement a relaxation phase via an NVT (constant atom Number, Volume, and Temperature) ensemble with the use of the Nosé-Hoober thermostat and barostat [14]. In this procedure, the structure reaches a temperature of 300K in 1 ps. Afterwards, equilibrium state is achieved with an NVE (constant atom Number, Volume, and Energy) ensemble for 1 ps to further relax the system at 300 K. Then we apply a shear force F, as shown in Fig. 1, to overcome static friction and produce motion. The applied force is increased gradually over time so that we can distinguish static and dynamic friction phases and measure the corresponding values. It is also worth mentioning here that all following results have been obtained by averaging over 10 simulations, with different initial atomic velocities, to account for the computational uncertainties.

[1] https://lammps.sandia.gov/

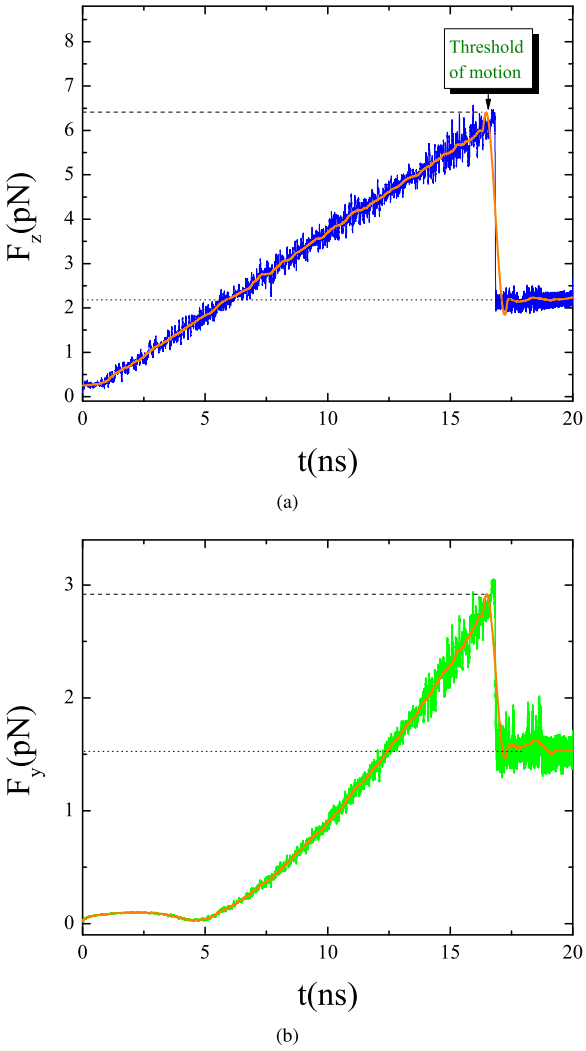

Fig. 2. Force components versus time (a) along z and (b) y directions (Normal force). Motion onset is indicated with a leader in (a). Dynamic phase follows the value jump depicted in both graphs.

3. Results and discussion

All lengths reported in this section are integer multiples of the hexagons in the CNT hexagonal lattice. Furthermore, the employed overlapping length d corresponds to the non-dimensional ratio of the overlapping length over the total CNT length.

Figure 2 depicts friction force components along z and y directions for an overlap of $d = 2/8 = 1/4$; see lower-left corner of Fig. 1 for the employed coordinate system. Solid lines, in the same figure, correspond to smoothed curve fitting to raw data. Although graphs in Fig. 2 represent a rather simplistic view of friction, they do agree fairly well with obtained experimental results of an object's movement on a flat surface. The increase of static frictional forces preventing relative motion, up to a certain threshold value, are recorded and this motion threshold is indicated with a leader in Fig. 2(a). This threshold of motion involves a manifestation of the stick-slip mechanism at both microscopic and macroscopic levels since it resembles the behavior exhibited by two surfaces in contact starting from rest and attempting to slide them with respect to each other. We can obviously use this point to evaluate the value of static friction coefficient; see dashed lines in Fig. 2. Past this point, the two CNTs are in relative motion and the frictional resistance exhibits a practically constant value correspond-

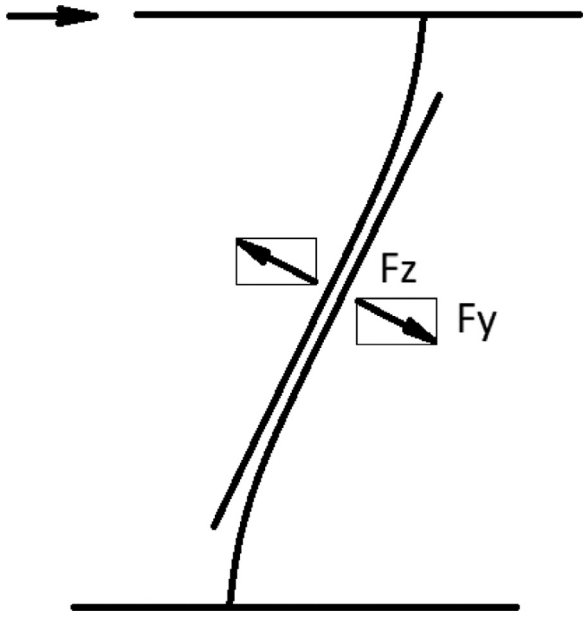

Fig. 3. Observed bending-dominated mechanism of CNT interaction, showing the resultant forces in the primary plane of interaction yz.

ing to the dynamic frictional forces; see dotted lines in Fig. 2. Specifically, for the static friction coefficient, based on the case shown in Fig. 2, we substitute $F_z^{smax} = 6.41$ pN and $F_y = 2.91$ pN in $F_z^{smax} = \mu_s F_y$ which yields $\mu_s = 2.20$ for the static case. Regarding now the dynamic case, we similarly substitute $F_z = 2.18$ pN and $F_y = 1.51$ pN to get $\mu_k = \frac{F_z}{F_y} = 1.44$. These results are obviously in qualitative agreement with the standard model of friction and the decreased value of the dynamic coefficient with respect to the static one .

We additionally perform the calculation of friction forces and corresponding coefficient values by considering an alternative setup. Specifically, we consider a constant speed for one of the layers (upper one) and compute resulting friction forces for all colliding CNT pairs with time. The values of the same force components (F_z, F_y and F_x) are illustrated in Fig. 4 versus time. Once again, solid lines correspond to a smoothed curved fit to the obtained readings. Due to the employed periodic boundary conditions along z axis, we capture several crossings of CNTs and transitions from static to dynamic friction. We observe and reason from basic principles that the dominant mechanism at play is bending: As CNTs try to occupy the same space, carbon atoms repel each other, causing a force component, F_z, that resists motion. As bending deformation of the CNTs progresses, another force component, F_y, develops in a direction perpendicular to the motion direction and the substrate plane Fig. 3. Lastly, beyond a certain deflection amount, the system becomes unstable and CNTs rapidly deflect sideways, i.e., in the x-

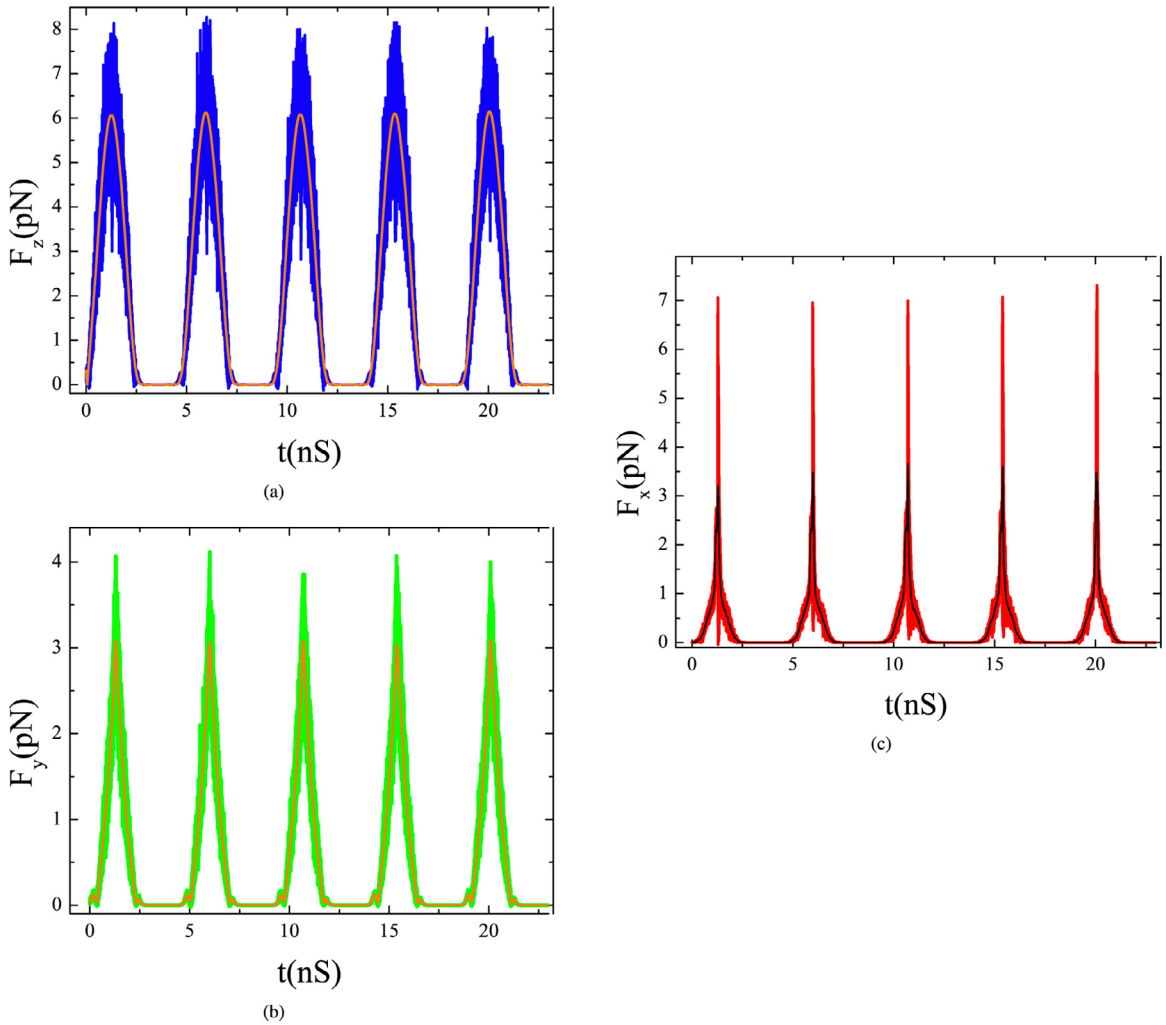

Fig. 4. Force components (a) along z, (b) y and (c) x directions versus time in dynamic case. Solid lines are the smoothed fitting to real data.

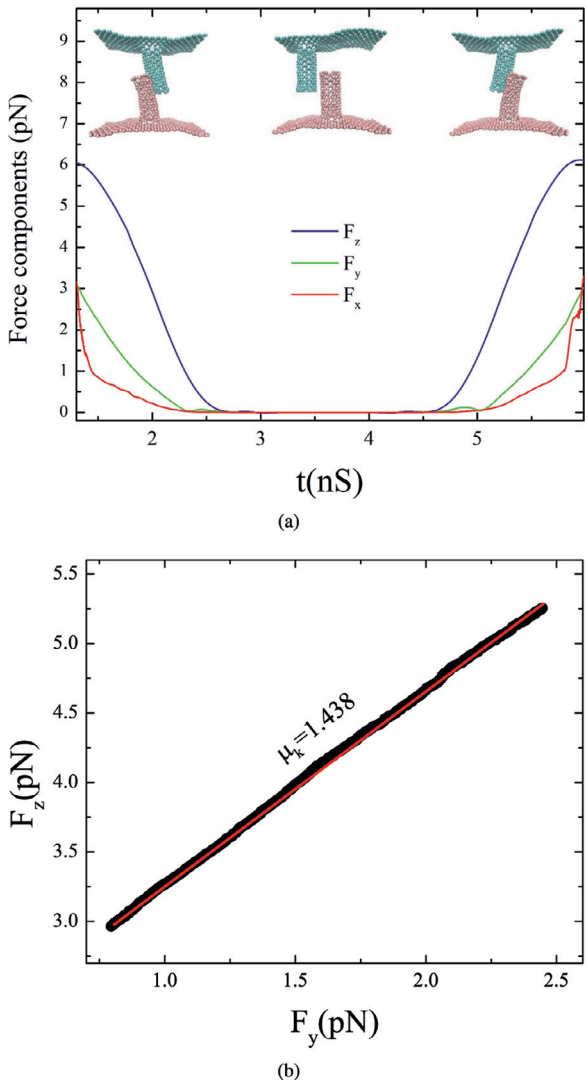

Fig. 5. (a) Force components are shown in one period. (b) Force component in the direction of movement (z axis) as a function of force in normal direction (y azis).

direction, to clear each other. In the special case in which CNTs contact each other centrally, as in this study, then a leftwards or rightwards x-deflection is equally possible.

During the relatively brief time interval of this resetting motion, a lateral force component, F_x, also appears, similarly to F_y, and then vanishes together with F_z and F_y, when CNTs are no longer in contact. In the context of multiple arrayed CNTs, undergoing similar motions with stochastic time interval differences, this mechanism as postulated will cause sustained resultants for F_z and F_y, while stochastically the F_x components would cancel each other out, due to their practically random leftward and rightward orientations. This behavior is very similar to the well-understood mechanism of friction between rough surfaces and it is precisely this similarity that allows us to compare the studied CNT contact with friction and describe it using a friction coefficient. This insight also opens the possibility to use CNTs in isolation or in patterned arrays to engineer desired frictional behaviors.

Force components for one period are depicted in one graph, Fig. 5(a). At the same time we overlay the position of CNTs to each other with respect to time so that we can easily identify the corresponding regions in the graph. We may now use the same equation we employed before, i.e., $F_z = \mu_k F_y$, and determine dynamic friction coefficient, μ_k, with the help of the average values for F_y

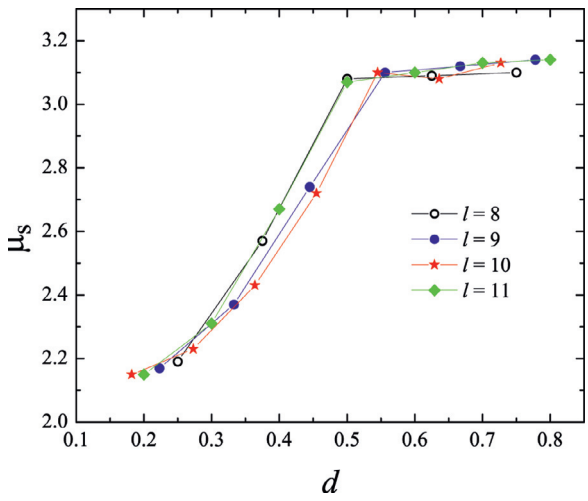

Fig. 6. Static friction coefficient, μ_s, as a function of the dimensionless overlapping length d for different CNTs dimensionless lengths, l. For all lengths, μ_s rapidly increases till $d \approx 0.5$ and it then slowly converges to its maximum value as $d \to 1$.

and F_z that correspond to the dynamic friction phase. Specifically, if we follow this procedure and plot the average values, $\bar{F}_z$ vs $\bar{F}_y$, on the same graph, we get the relation depicted in Fig. 5(b). This graph, which corresponds to the same dimensionless overlapping length used in Fig. 2, allows us to estimate the dynamic friction coefficient, μ_k, as 1.438. The dynamic friction coefficient value calculated by this method is approximately equal to the value derived before.

We now proceed with the investigation of the effect of the aforementioned factors on the frictional coefficient values. We start with the effect of CNTs overlap on the static friction coefficient. Figure 6 depicts the static friction coefficient value as a function of the dimensionless overlap length d for different dimensionless length of CNTs l. This behavior is in agreement with the static friction coefficient results reported by Suekane et al. in [7]. Specifically, they experimentally measured the static friction force for a wide range of overlap lengths and acquired results in the range of (2,3) for the static friction coefficient value for overlapping lengths up to 60 nm. As can be easily seen in Fig. 6, we obtain results with practically the same range of values. Another interesting finding in Fig. 6 is the abrupt increase in the value of the coefficient for overlap values, d, between 0.25 and 0.5, followed by a very slow increase for higher overlap ratios. The abrupt increase in the value of the friction coeent, for $0.25 < d < 0.5$ is attributed to the increasing bending stiffness of the CNTs, as the median contact point moves closer to their foundation, but for $d > 0.5$ the stiffness is sufficiently high that even minor perturbations cause an early lateral deflection of the CNTs, thereby shifting the contact point sideways rather than further downwards, causing an apparent æsaturationg of the mechanical effect. Consequently, an asymptotic trend is observed for $d > 0.5$.

The dynamic friction coefficient as a function of relative speed of CNTs pair for a range of overlapping lengths is depicted in Fig. 7(a). According to the standard model of friction, dynamic friction remains constant between two surfaces, regardless of the relative speed of their movement. In Fig. 7(b) we can observe that dynamic friction coefficient values converge to a practically constant value for each examined relative speed of CNTs, when the overlap ratio exceeds 3/8.

To better illustrate this result, we plot the F_z and F_y component values with time under the lowest and highest considered speeds, in Fig. 8(a) and (b), respectively. Both graphs correspond to an overlap ratio of 2/8 and we can observe a slight decrease in both

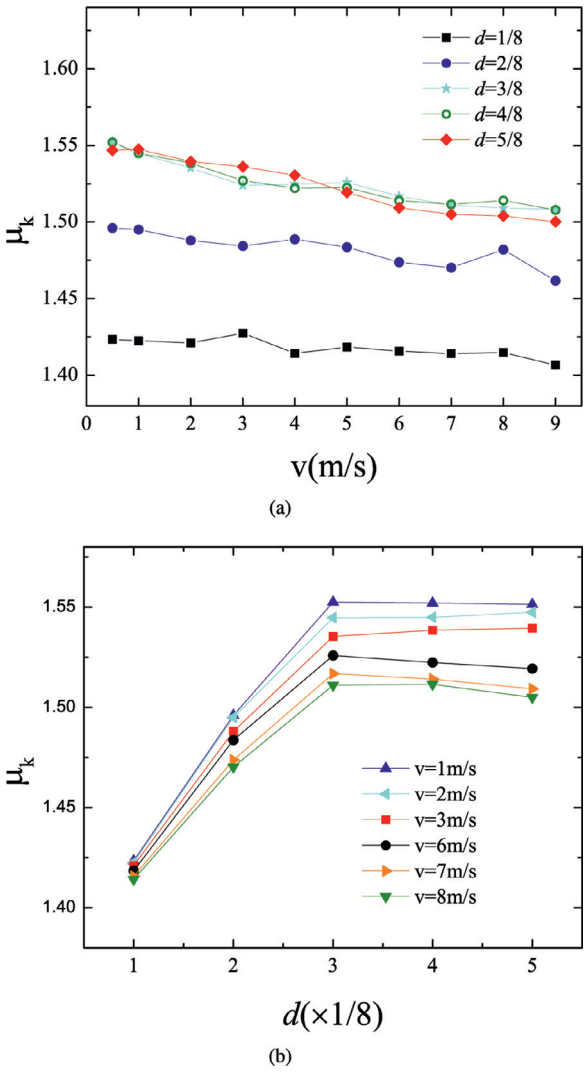

Fig. 7. Dynamic friction coefficient as a function of relative speed of CNTs for different overlapping lengths.

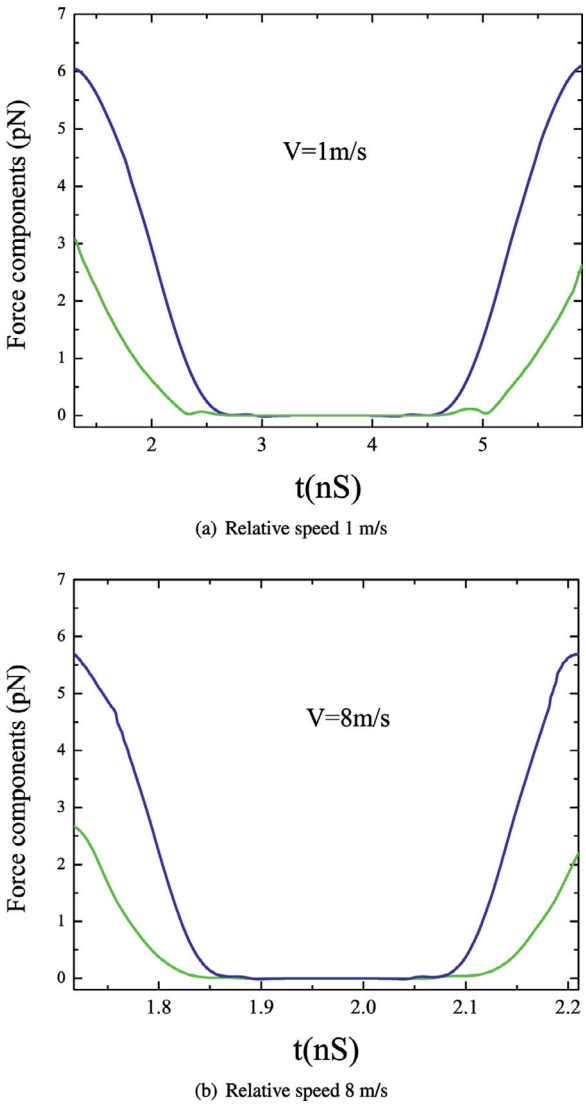

Fig. 8. Force components along z (blue) and y (green) directions versus time in one period for an overlap of $d = 2/8$. (Color online)

component values for the highest speed of relative movement. The calculated difference is less than 1% for the depicted ratio, $d = 2/8$, and it goes up to 2% for higher interlocking values. This drop is due to inertial effects of the deforming CNTs and is consistent with established trends in conventional materials, where likewise a very small drop in the dynamic friction coefficient is known to occur with increasing velocities -although not exactly for the same reasons; see [15,16].

4. Conclusions

In this study, we performed non-equilibrium molecular dynamics simulations to computationally estimate the values of static and dynamic friction coefficients between a pair of SWCNTs. We have considered two carbon nanotubes grown vertically each on a separate flat graphene substrate. Movement was induced by application of shear force on one of the layers and two separate approaches were employed for the calculation of friction coefficients. Both static and dynamic friction coefficient calculations resulted in large values of friction between the CNTs. Specifically, a value of approximately 3 is evaluated for the static friction coefficient with an overlapping ratio $d \geq 0.5$. The dynamic friction coefficient was calculated in the range of (1.4,1.5) for all overlapping lengths. Finally, we studied the effect of shear force, relative speed of movement and overlapping length on the friction coefficients' values with results that are largely aligned with experimental results and theoretical expectations.

It is observed and explained from basic principles that the phenomenon is bending-dominated, as CNTs deform when trying to occupy the same space. The overall manner of force generation bears similarity to the friction mechanism between rough surfaces, but with the additional affordance that a high, user-adjustable coefficient of friction is attainable.

Our measurements of friction forces between sliding pairs of CNTs can therefore shed some light into the properties of interaction between arrays of aligned CNTs grown on relevant substrates. Based on these insights, one may devise testing approaches for validating and experimentally acquiring relevant results. For example, aligned CNT arrays with low site density can be used in conjunction with an Atomic force microscope (AFM) to characterize single CNT behavior. On the other hand, a pair of CNT forests grown on substrate and sliding in respect to each other may be used for considering friction forces at the macroscopic scale.

Finally, some rather obvious next steps in this line of work include the study of potential temperature effects on friction coefficients along with the extension of our calculations to MWCNTs.

Declaration of Competing Interest

The authors declare that they have no known competing financial interests or personal relationships that could have appeared to influence the work reported in this paper.

Acknowledgements

This work has been funded by the following Nazarbayev University Collaborative Research Projects (CRPs):

1. “Development of smart passive-active multiscale composite structure for earth Remote Sensing Satellites (RSS) of ultrahigh resolution (ULTRASAT)”, Grant Award Nr.091019CRP2115, and 2. “Rapid response fixed astronomical telescope for gamma ray burst observation (RARE)”, Grant Award Nr. 091019CRP2101.

References

[1] D. Han, H. Mei, S. Xiao, W. Xue, Q. Bai, L. Cheng, CNT/SiC composites produced by direct matrix infiltration of self-assembled CNT sponges, J. Mater Sci. 52 (2017) 8401–8411.
[2] M. Chen, Design of an efficient flake powder metallurgy route to fabricate CNT/6061Al composites, Mater. Des. 142 (2018) 288–296.
[3] H.J. Qi, K.B.K. Teob, K.K.S. Lauc, M.C. Boycea, W.I. Milneb, J. Robertsonb, K.K. Gleasonc, Determination of mechanical properties of carbon nanotubes and vertically aligned carbon nanotube forests using nanoindentation, J. Mech. Phys. Solids 51 (2003) 2213–2237.
[4] H. Mori, Y. Hirai, S. Ogata, S. Akita, Y. Nakayama, Chirality dependence of mechanical properties of single-walled carbon nanotubes under axial tensile strain, Jpn. J. Appl. Phys. 44 (2005) L1307–L1309.
[5] S. Akita, H. Nishijima, T. Kishida, Y. Nakayama, Influence of force acting on side face of carbon nanotube in atomic force microscopy, Jpn. J. Appl. Phys. 39 (2000) 3724–3727.
[6] M.F. Yu, O. Lourie, M.J. Dyer, K. Moloni, T.F. Kelly, R.S. Ruoff, Strength and breaking mechanism of multiwalled carbon nanotubes under tensile load, Science 287 (2000) 637–640.
[7] O. Suekane, A. Nagataki1, H. Mori1, Y. Nakayama, Static friction force of carbon nanotube surfaces, App. Phys. Exp. 1 (2008). 064001-3
[8] H. Kinoshita, I. Kume, M. Tagawa, N. Ohmae, High friction of a vertically aligned carbon-nanotube film in microtribology, Appl. Phys. Lett. 85 (2004) 2780–2781.
[9] J. Servantie, P. Gaspard, Rotational dynamics and friction in double-walled carbon nanotubes, Phys. Rev. L. 97 (2006). 186106-4
[10] P. Liu, Y.W. Zhang, Translational dynamic friction analysis of double-walled carbon nanotubes, Mol. Sim. 37 (2011) 84–89.
[11] G.K. Dimitrakakis, E. Tylianakis, G.E. Froudakis, Pillared graphene: a new 3-D network nanostructure for enhanced hydrogen storage, Nano Lett. 8 (2008) 3166.
[12] L. Lindsay, D.A. Broido, Optimized Tersoff and Brenner empirical potential parameters for lattice dynamics and phonon thermal transport in carbon nanotubes and graphene, Phys. Rev. B 81 (2010). 205441-6
[13] S. Plimpton, Fast parallel algorithms for short-range molecular dynamics, J. Comput. Phys. 117 (1995) 1–19, doi:10.1006/jcph.1995.1039.
[14] S. Melchionna, G. Ciccotti, B.L. Holian, Hoover NPT dynamics for systems varying in shape and size, Mol. Phys. 78 (1993) 533–544.
[15] M.D. Bryant, On constitutive relations for friction from thermodynamics and dynamics, J. Tribol. 138 (2016). 041603-8
[16] B.N.J. Persson, U. Tartaglino, O. Albohr, E. Tosatti, Rubber friction on wet and dry road surfaces: the sealing effect, Phys. Rev. B 71 (2005). 035428-8.